

Supporting Information

Sequence liquid manipulation on a multifunctional snowflake-patterned interface with dual unidirectional wettability

Weiming Wu,^a Haoyu Bai,^b Yi Yang,^a Guoqiang Li,^{*a} Zuqiao Chen,^a Chengning Tang,^a Huan Yin,^a Lin Lai,^a Jiasong Liu,^a Sensen Xuan,^a Yuegan Song,^a Senyun Liu,^c Kai Yin^{*d} and Moyuan Cao^{*b}

This file contains 11 supporting figures and 6 movies.

Supporting Movies:

Movie S1. The water droplet (5 μL) was released to one end of the rectangular symmetric channel, and the droplets could transport from the right end of the rectangular symmetric channel to the circular water storage tank at the left end.

Movie S2. The water droplet (5 μL) was transported from the right end of the asymmetrical wedge to the circular water storage tank at the left end.

Movie S3. The water droplet (5 μL) touched the hydrophobic side, it rapidly penetrated the superhydrophilic side in a direction and formed a water film.

Movie S4. The ion exchange resin can be dislodged by slight mechanical vibration for recovery.

Movie S5. Interfacial reaction process between fog containing calcium ion and hydrogen ion exchange resin solution on MSPI.

Movie S6. The plant incubator can collect water from the fog for fixed-point irrigation.

Supporting Figures:

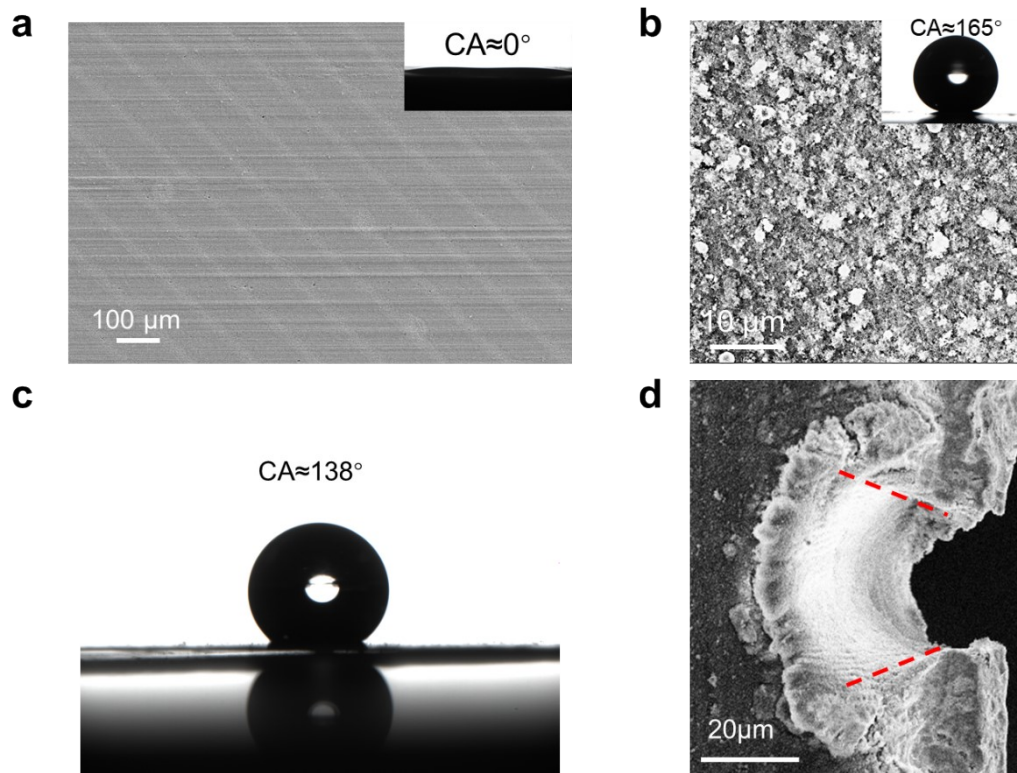


Fig. S1 Characterization of the MSPI. (a) Construction of periodic stripe structure on aluminum sheet surface by femtosecond laser. (b) SEM image and contact angle of superhydrophobic area. (c) The contact angle of the unprocessed modified aluminum sheet. (d) The asymmetric conical structure of the micro-hole was constructed by femtosecond laser.

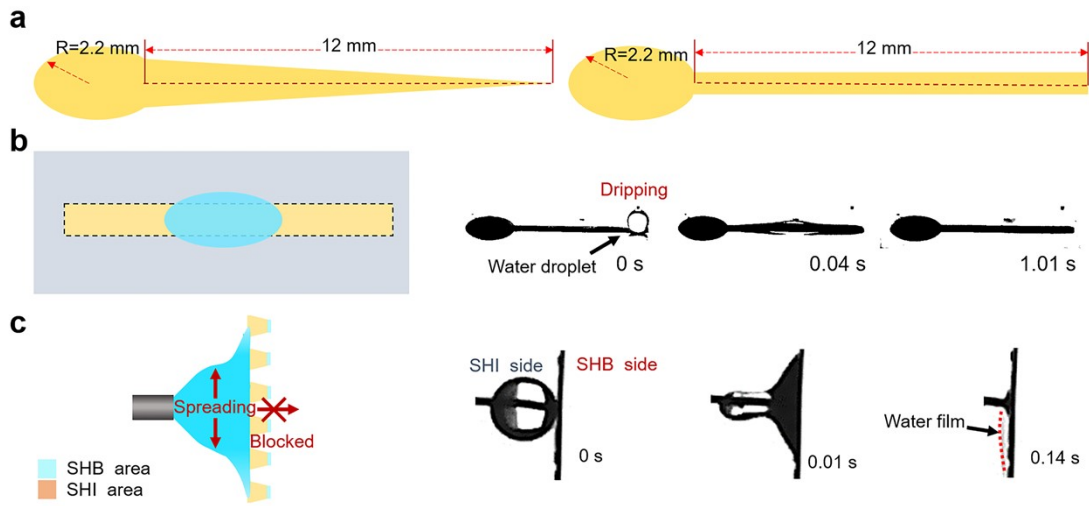


Fig. S2 Model design and droplet transport process. (a) Dimensions of a circular water storage area connected with a rectangular symmetrical channel and a wedge-shaped asymmetric channel with a circular water storage area were designed. Schematic diagram of droplet transport on (b) rectangular symmetric channel and c) micro-hole array.

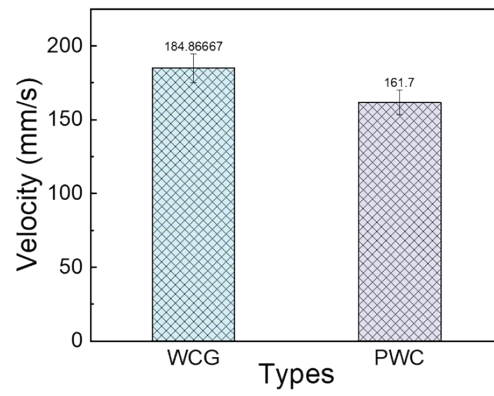


Fig. S3 Comparison of droplet transport velocities in a wedge channel with microgrooves (WCG) and a planar wedge channel (PWC).

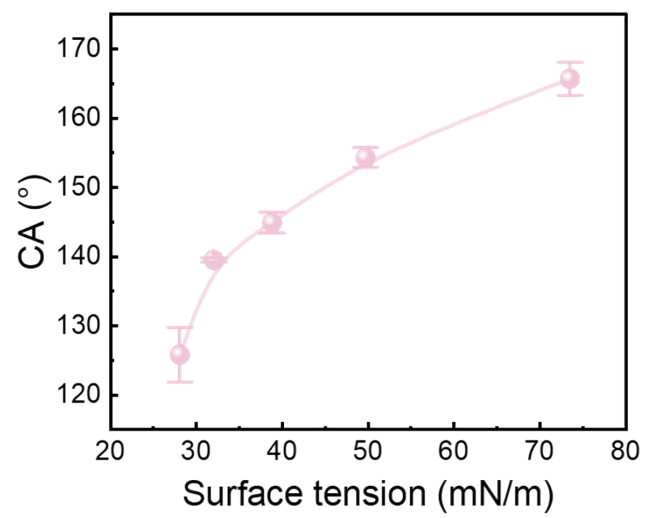


Fig. S4 Contact angle characterization of liquids with different surface tensions.

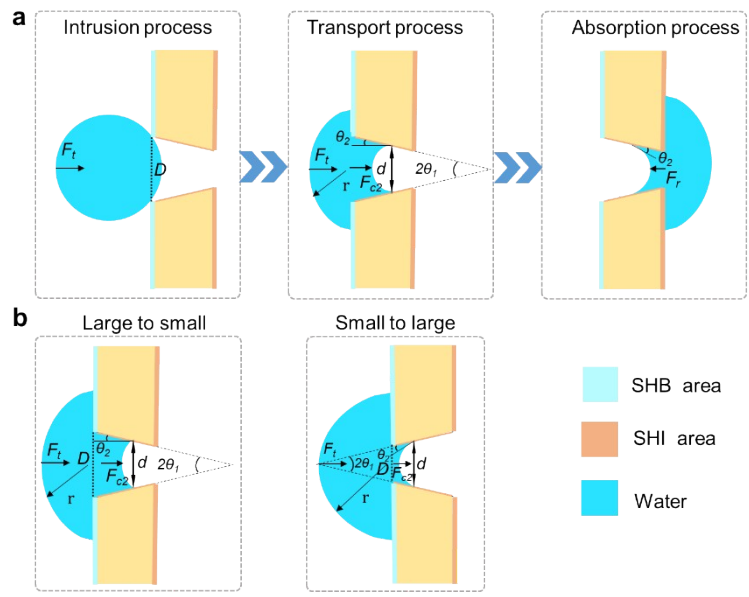


Fig. S5 Transport model of water droplets in micro-hole. (a) The transportation of water droplets through micro-hole. (b) Transport analysis of water droplets in two modes.

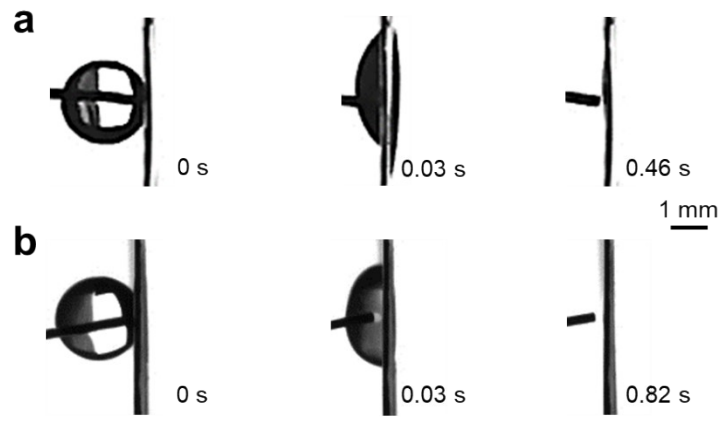


Fig. S6 Transportation process of water droplet in (a) LTS micro-hole array and (b) STL micro-hole array.

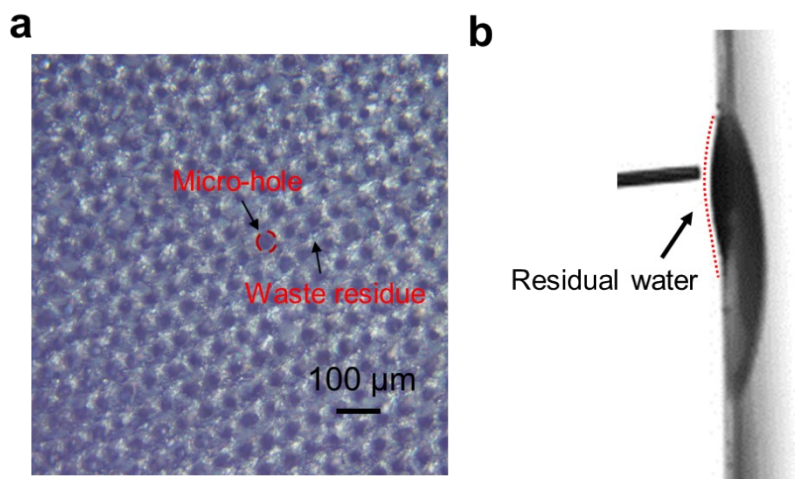


Fig. S7 (a) Morphology and (b) droplet transport effect of the micro-hole array with 60 μm hole spacing.

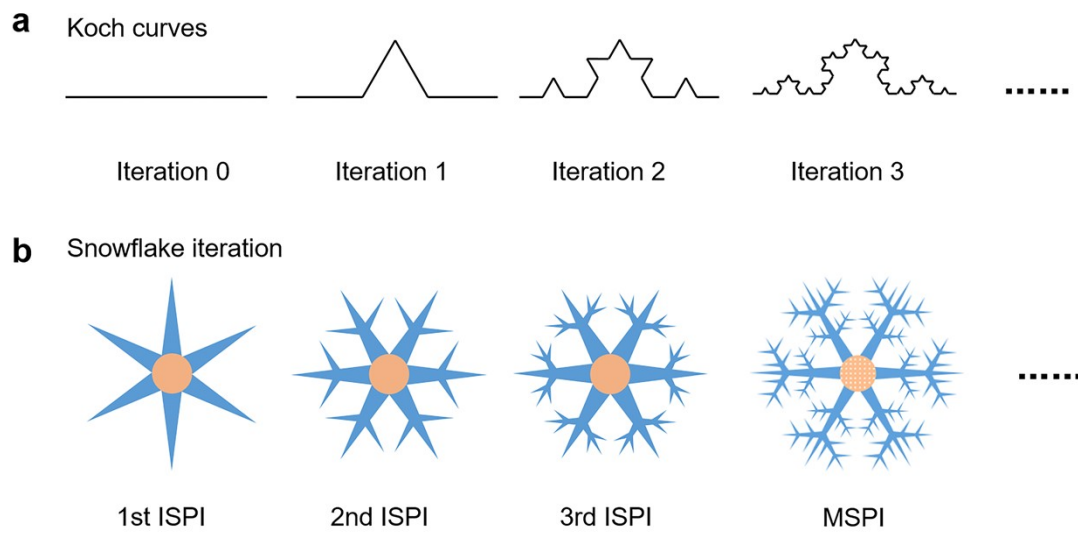


Fig. S8 Fractal design of the multifunctional snowflake-patterned interface. (a) Fractal theory of Koch snowflake. (b) Based on the fractal iterative principle, the first iteration snowflake-patterned interface (1st ISPI), the second iteration snowflake-patterned interface (2nd ISPI), the third iteration snowflake-patterned interface (3rd ISPI), and the MSPI were designed.

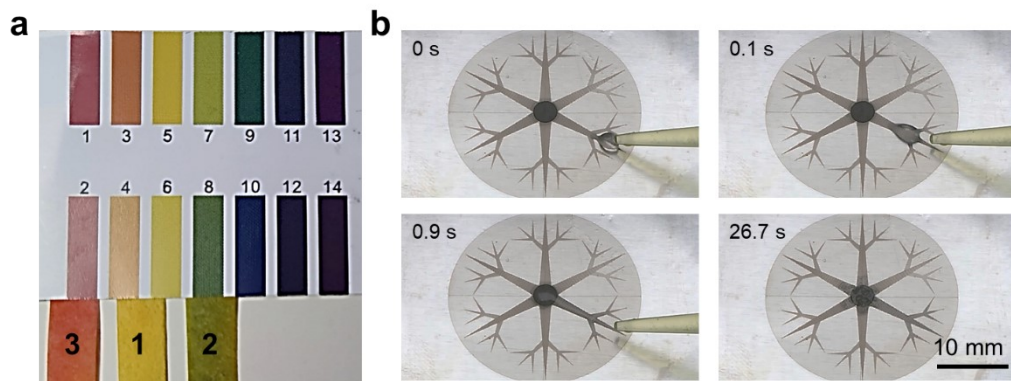


Fig. S9 (a) pH characterization of reactants and products. The hydrogen ion exchange resin suspension solution, the calcium chloride solution, and the generated liquid are marked as serial numbers 1, 2, and 3, respectively. (b) Transport and separation process of hydrogen ion exchange resin suspension solution on MSPI.

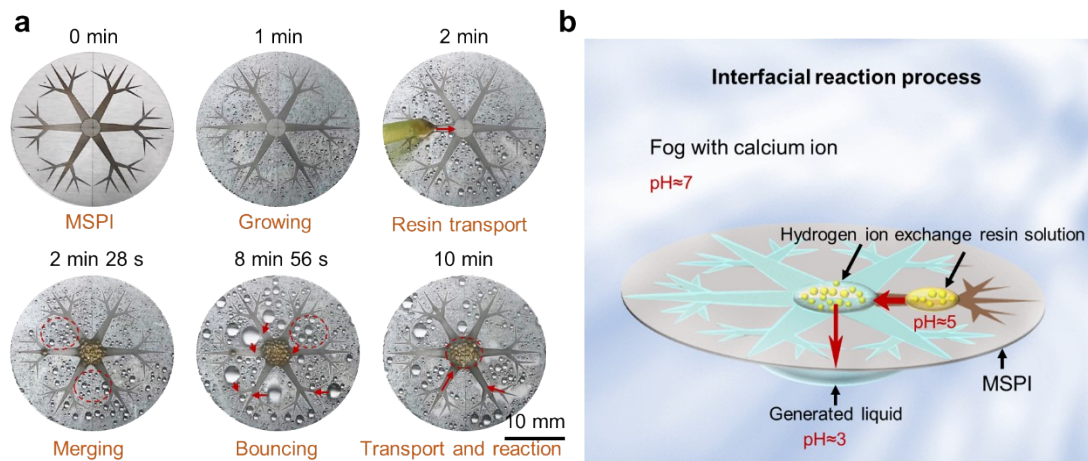


Fig. S10 (a) Interfacial reaction process between fog containing calcium ion and hydrogen ion exchange resin solution on MSPI and (b) Schematic diagram of reaction result.

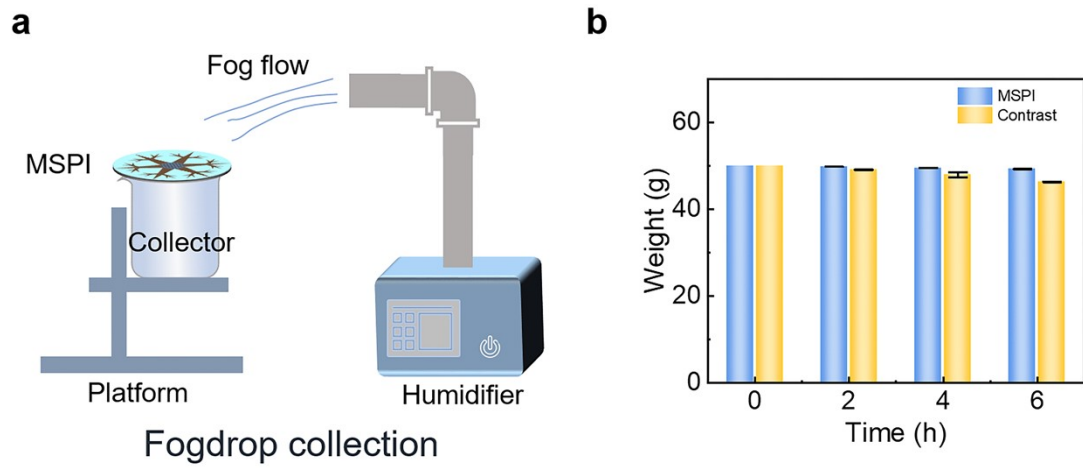


Fig. S11 Application of fog collection. (a) Schematic diagram of fog collection experiment. (b) Comparison of water storage capacity between closed plant incubator and open fog collector.